engineering proceedings

MDPI

Proceeding Paper

Transient Numerical Simulation of Reheating Furnace Behavior for Continuous Casting Rail Steel Blooms Prior to Rolling †

Jan Rybář [1,*], Sohaibullah Zarghoon [1,2], Sardar Maroofi [2], Sayed Yousuf Sayed [2], Stanislav Ďuriš [1], Ibrahim Shaikh [3] and Peter Onderčo [1]

[1] Institute of Automation Informatizationand Measurement, Faculty of Mechanical Engineering, Slovak University of Technology in Bratislava, Námestie Slobody 17, 812 31 Bratislava, Slovakia; sohaibullah.zarghoon@stuba.sk (S.Z.); stanislav.duris@stuba.sk (S.Ď.); peter.onderco@stuba.sk (P.O.)

[2] Department of Auto Mechanical Engineering, Faculty of ElectroMechanic, Kabul Polytechnic University, Kart-e Mamorin, District 5, Kabul 1001, Afghanistan; sardar.maroofi@kpu.edu.af (S.M.); s.yousuf@kpu.edu.af (S.Y.S.)

[3] Department of Automation and Control Engineering, Faculty of Applied Informatics, Tomas Bata University in Zlín, Nad Stráněmi 4511, 760 05 Zlín, Czech Republic; shaikh@utb.cz

* Correspondence: jan.rybar@stuba.sk

† Presented at the 15th International Scientific Conference TechSys 2026—Engineering, Technologies and Systems, Plovdiv, Bulgaria, 14–16 May 2026.

Abstract

In this study a transient finite element model was developed to examine the temperature evolution of continuous casting blooms during reheating prior to rail rolling. The simulation was carried out using COMSOL Multiphysics 5.6, incorporating convective and radiative heat transfer mechanisms under a three-zone furnace (preheating, heating and soaking) temperature schedule. The temperature distribution and soaking uniformity were evaluated over a 7200 s heating cycle. The results indicate that proper adjustment of furnace setpoints enables the bloom center to reach approximately 1220 °C while maintaining acceptable temperature uniformity $\Delta T \leq 50$ °C. This study shows how numerical modeling can be used to improve thermal homogeneity prior to hot rolling and optimize reheating furnace performance.

Keywords: heat distribution; heat transfer; finite element analysis; rail steel blooms; reheating furnace; soaking uniformity

1. Introduction

The reheating of continuous casting rail steel blooms is a crucial stage in rail steel manufacturing, directly influencing rolling behavior, microstructural evolution, and final mechanical performance. Prior to hot rolling, blooms must reach a sufficiently high and uniform temperature to ensure stable plastic deformation and minimize internal thermal stresses. Inadequate soaking may result in temperature gradients between the surface and core, leading to uneven deformation, increased rolling loads, and reduced product quality [1,2]. Heat transfer inside reheating furnaces is governed primarily by radiative and convective mechanisms, coupled with transient heat conduction within the steel. Because carbon steel exhibits temperature-dependent thermophysical properties, accurate prediction of internal temperature evolution requires numerical modeling rather than analytical approximation. The finite element method has been widely employed to simulate slab and bloom reheating processes under industrial furnace conditions [3–5]. A schematic representation of the reheating furnace configuration considered in this study is shown in

Check for updates

Academic Editors: Nikola G. Shakev, Valyo N. Nikolov, Nikolay R. Kakanakov and Sevil A. Ahmed-Shieva

Published: 24 July 2026

Copyright: © 2026 by the authors. Licensee MDPI, Basel, Switzerland. This article is an open access article distributed under the terms and conditions of the Creative Commons Attribution (CC BY) license.

Figure 1. The furnace consists of three thermal zones: preheating, heating, and soaking. The continuous casting bloom enters the furnace and moves continuously through these zones, where it is exposed to high-temperature combustion gases and radiative heat flux from burners positioned above and below the bloom.

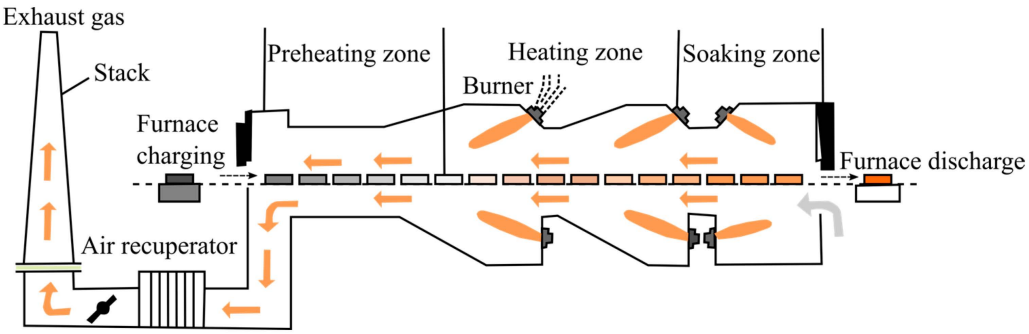


Figure 1. Illustration of the longitudinal section of a rail bloom reheating furnace.

Heat transfer occurs predominantly by radiation at elevated temperatures, while convection contributes additional surface heating. During the final soaking zone, the bloom is maintained at a nearly constant furnace temperature for sufficient residence time to reduce internal thermal gradients and achieve temperature homogenization prior to rail rolling. Although numerous investigations have addressed slab reheating in walking beam and pusher-type furnaces [3,4], limited attention has been devoted specifically to thermal homogenization of rail steel blooms and quantitative evaluation of soaking effectiveness prior to rolling. In particular, the influence of temperature-dependent material properties on discharge temperature uniformity has not been extensively discussed in the context of rail production. In the present study, a transient two-dimensional finite element model is developed using COMSOL Multiphysics to simulate the reheating process of continuous casting rail steel blooms. The model incorporates convective and radiative boundary conditions together with temperature-dependent thermophysical properties of carbon steel. Temperature evolution during preheating, heating, and soaking zones is analyzed, and soaking effectiveness is evaluated using the maximum–minimum temperature difference ($\Delta \boldsymbol{T}$) at discharge. The developed model provides a numerical framework for assessing reheating furnace schedules and improving thermal homogenization in rail steel manufacturing.

2. Methodology

2.1. Physical Model and Geometry

A two-dimensional transient heat transfer model was developed to simulate the reheating process of a continuous casting rail steel bloom prior to rolling (Figure 2).

The bloom cross-section was modeled as a rectangular domain with dimensions 0.35×0.25 m. Due to the large length-to-thickness ratio of industrial blooms and the dominance of transverse heat transfer during reheating, a 2D cross-sectional approach was considered sufficient to capture internal temperature evolution. The reheating process was divided into three furnace zones as mentioned in the Introduction. The bloom was assumed to move continuously through these zones following a prescribed time-dependent furnace temperature schedule over a total heating time of 7200 s.

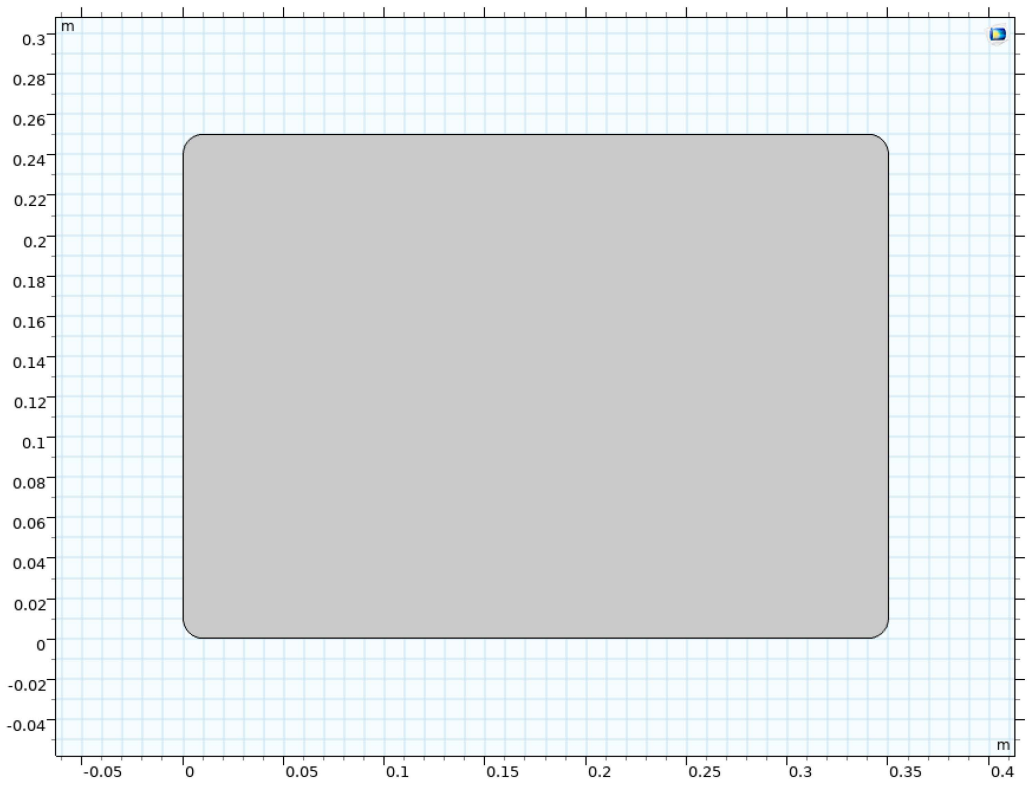


Figure 2. 2D cross−section of rail steel bloom.

2.2. Governing Equation

Transient heat conduction inside the steel bloom was described using the heat equation:

$$\rho C_p(T)\frac{\partial T}{\partial t} = \nabla \cdot (k(T)\nabla T) \quad (1)$$

According to Equation (1), the net heat passed into the material (right side) equals the rate of heat stored inside the material (left side). Thermal energy accumulation is expressed as $\rho C_p(T)\frac{\partial T}{\partial t}$, where $\rho(T)$ denotes the temperature-dependent density and $C_p(T)$ is the temperature-dependent specific heat capacity. Fourier's law states that heat conduction is represented by the expression $\nabla \cdot (k(T)\nabla T)$, where $k(T)$ is the temperature-dependent thermal conductivity. The equation becomes nonlinear because $\rho(T)$, $C_p(T)$, and $k(T)$ change with temperature, which is crucial in simulations of reheating furnaces where the rail steel bloom undergoes significant temperature fluctuations [6]. To solve the transient heat equation, a time-dependent study was used in COMSOL Multiphysics. The rail steel bloom geometry is meshed into small elements, and COMSOL automatically approximates the temperature at each element using interpolation functions. The software internally converts the equation into its integral form and assembles a system of algebraic equations, which it solves to compute the temperature distribution throughout the rail steel bloom over time.

2.3. Material Properties

The bloom material was assumed as carbon rail steel. Density, thermal conductivity, and specific heat were defined as temperature-dependent functions based on the interpolation of data from the literature [6]. Surface emissivity was analyzed using two approaches: a constant value to approximate an oxidized steel surface under furnace conditions, and a temperature-dependent formulation based on data from the literature [6]. The temperature-dependent approach was adopted in the final model, as it provides a

more accurate representation of radiative heat transfer by accounting for the variation in emissivity with temperature.

2.4. Boundary Conditions

Heat transfer at the bloom surface was modeled considering both convective and radiative modes. The convective heat flux is expressed as Equation (2) [6,7]:

$$q_{conv} = h\left(T_{gas}(t) - T\right) \tag{2}$$

where h is the convective heat transfer coefficient, $T_{gas}(t)$ is the time-dependent furnace gas temperature, and T is the bloom surface temperature. Radiative heat transfer is described by Equation (3).

$$q_{rad} = \varepsilon(T)\sigma\left(T_{gas}^4(t) - T^4\right) \tag{3}$$

where $\varepsilon(T)$ is the surface emissivity of the bloom, σ is the Stefan–Boltzmann constant, and T_{gas} is the furnace gas temperature [8]. The total heat flux at the bloom surface can be expressed as Equation (4) [9]:

$$q_{total} = q_{conv} + q_{rad} \tag{4}$$

The furnace temperature schedule was divided into three zones with time limitation: preheating (0–1800 s), heating (1800–5400 s), and soaking (5400–7200 s). The initial rail steel bloom temperature was set to 900 °C according to hot-charge conditions to reflect its entry temperature into the furnace.

The transient heat conduction problem with coupled convective and radiative boundary conditions was modeled in COMSOL using the finite element method. Convective and radiative fluxes, as described in Equations (2) and (3), were applied as boundary conditions at the rail steel bloom surface, with the time-dependent furnace gas temperature T_{gas} specified accordingly. The temperature distribution within the rail steel bloom was computed over time by solving the heat equation (Equation (1)) across all mesh elements, accounting for the combined effects of convection and radiation.

2.5. Numerical Implementation

The model was implemented in COMSOL Multiphysics using the heat transfer in the solid interface with a time-dependent solver to simulate the heating of the rail steel bloom cross-section over time. A combined mesh strategy was used, and a boundary layer mesh was applied near the boundaries to capture the strong temperature gradients that develop during the early stages of heating, while the interior was discretized with a coarser free triangular mesh to reduce computational cost (Figure 3) [10].

The simulation covered a time interval of 0–7200 s, and the results were analyzed through several post-processing methods. Surface temperature plots were generated at selected times (1800 s, 4500 s, and 7200 s) to visualize the temperature distribution across the cross-section, while the evolution of the core temperature was tracked to assess heating at the center. Temperature profiles across the bloom width were examined to identify any uneven heating, and soaking uniformity at the discharge time was evaluated using the temperature difference $\Delta T = T_{max} - T_{min}$, where T_{max} and T_{min} represent the maximum and minimum temperatures within the cross-section. Smaller ΔT values indicate more uniform heating, which is essential for subsequent processing steps.

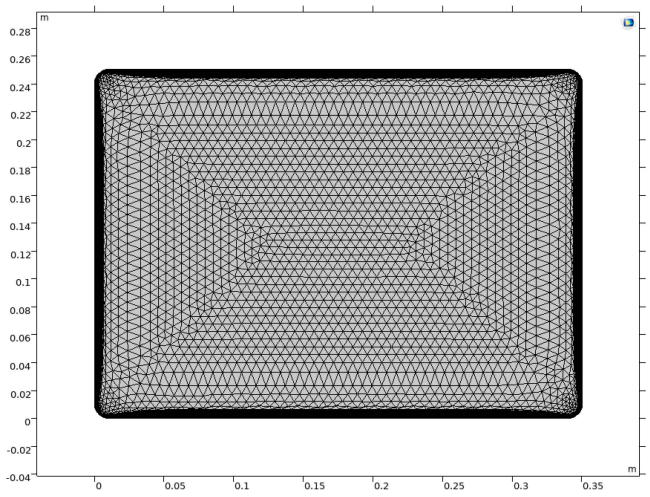


Figure 3. Mesh used for the rail steel bloom cross−section.

3. Results and Discussion

3.1. Temperature Field Evolution

Figures 4–6 presents the temperature distribution within the rail steel bloom cross-section at three selected times. During the preheating zone (1800 s; Figure 4), a pronounced temperature gradient is observed between the surface and the core, indicating rapid surface heating dominated by radiation. At 4500 s, corresponding to the heating zone (Figure 5), the internal temperature increases significantly and the gradient decreases as heat diffuses toward the bloom center. The surface temperature approaches the furnace gas temperature, while the core continues to rise due to conductive heat transfer. At the end of the soaking stage (7200 s; Figure 6), the temperature field becomes nearly uniform, demonstrating effective thermal homogenization.

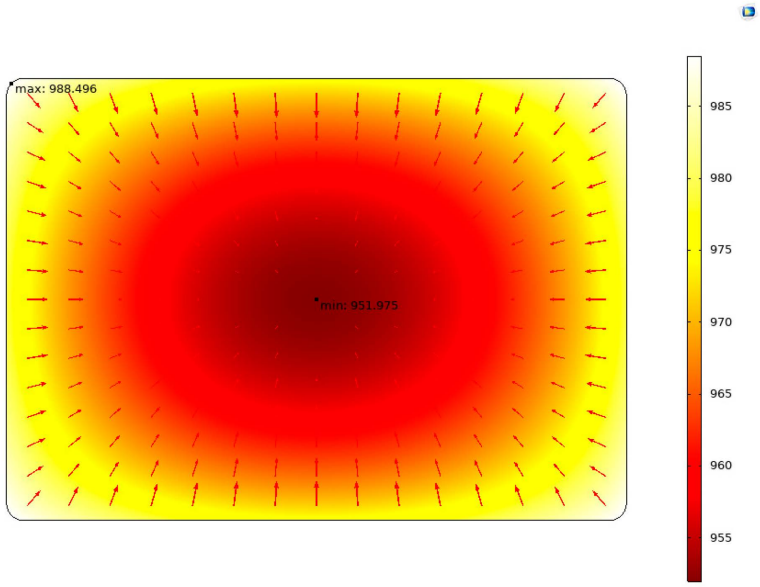


Figure 4. Temperature distribution across the bloom cross-section at 1800 s (preheating zone).

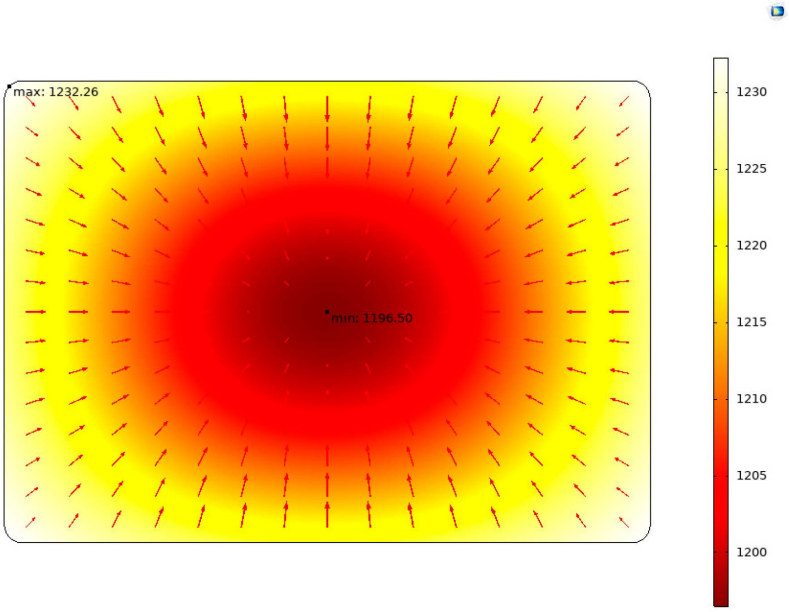


Figure 5. Temperature distribution across the bloom cross-section at 4500 s (heating zone).

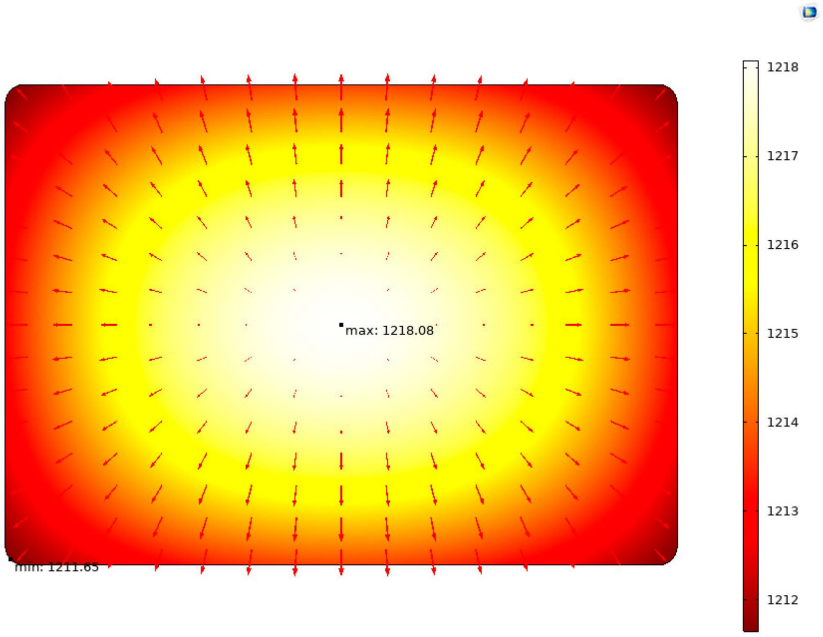


Figure 6. Temperature distribution across the bloom cross-section at 7200 s (soaking zone).

3.2. Core Temperature Evolution

Figure 7 illustrates the temperature evolution at the rail steel bloom center. The core temperature increases gradually during the preheating zone and more rapidly during the heating zone. During soaking, the rate of increase decreases as the temperature approaches equilibrium with the furnace environment. The final core temperature reaches approximately 1220 °C, satisfying typical rail rolling requirements.

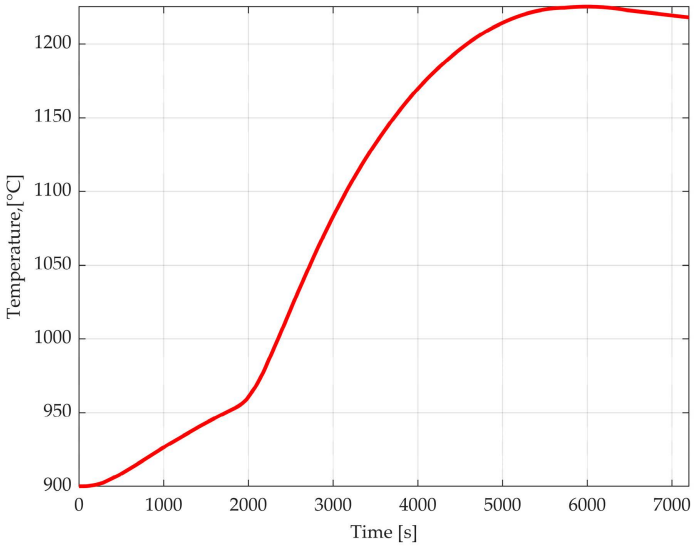


Figure 7. Core temperature evolution at the rail steel bloom center during preheating, heating, and soaking zones.

3.3. Temperature Distribution from Surface to Core

Figure 8 shows the location of six equally spaced measurement points across the rail steel bloom cross-section, from the surface to the core. Temperature histories at these points are presented in Figure 9, revealing the transient thermal behavior during all three zones. The surface heats fastest due to direct exposure to radiative flux, while the inner layers exhibit delayed heating. Figure 10 shows the corresponding temperature fields at selected times, illustrating how heat diffuses from the surface toward the core. As soaking progresses, all temperature curves in Figure 9 converge, confirming internal thermal diffusion and the reduction in spatial temperature gradients.

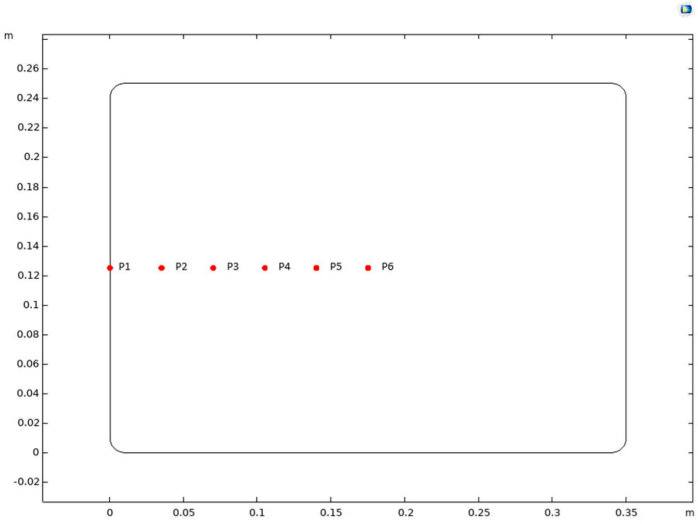


Figure 8. Location of six equally spaced measurement points across the bloom cross-section from surface to core, used for monitoring temperature evolution.

https://doi.org/10.3390/engproc2026150076

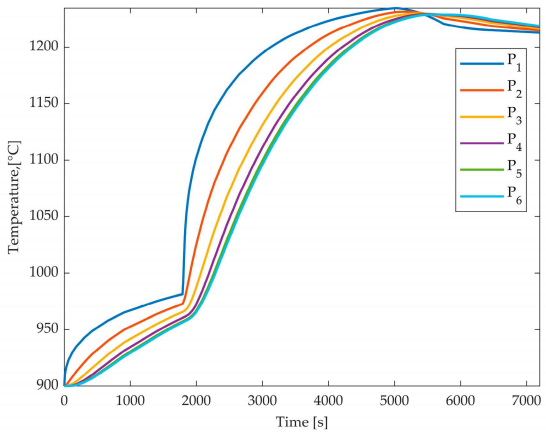


Figure 9. Temperature histories at six points during preheating, heating, and soaking zones.

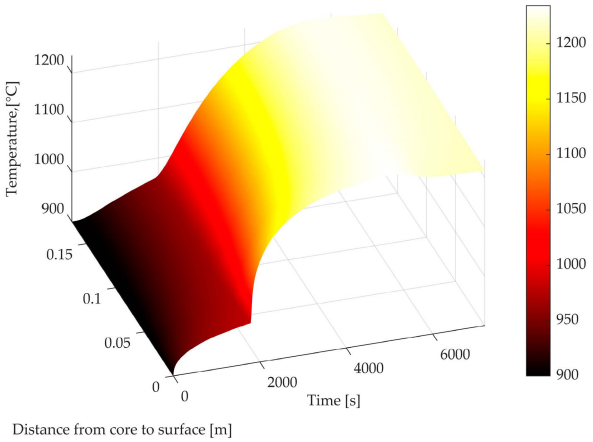


Figure 10. 3D temperature field of the rail steel bloom cross-section at selected times.

3.4. Soaking Uniformity Evaluation

At the end of the soaking zone (7200 s), the maximum and minimum temperatures within the rail steel bloom were found to be:

$$T_{max} \approx 1218.08\ ^{\circ}\mathrm{C} \tag{5}$$

$$T_{min} \approx 1211.65\ ^{\circ}\mathrm{C} \tag{6}$$

Resulting in $\Delta T = (5) - (6) = 6.43\ ^{\circ}\mathrm{C}$, this temperature difference indicates excellent thermal homogenization suitable for rail rolling operations. Interestingly, the maximum temperature occurs near the bloom center, while slightly lower temperatures are observed near the surface corners. This phenomenon results from transient thermal equilibration during soaking. As surface heating stabilizes and conductive diffusion continues inward, slight temperature inversion may occur, leading to a marginally higher core temperature. Such behavior is physically plausible and indicates sufficient soaking time.

3.5. Influence of Temperature-Dependent Properties

Comparison between constant and temperature-dependent material properties (Figure 11) shows that incorporating realistic thermophysical variations increases predicted temperature gradients and produces more accurate results. The temperature-dependent model yields a slightly higher ΔT, with steeper surface gradients and a larger core-to-surface temperature difference, especially at elevated temperatures. Radiation remains the dominant heat transfer mechanism during reheating, particularly in the heating zone. Varia-

tions in emissivity strongly affect the heating rate and final discharge temperature. Overall, combining temperature-dependent properties with radiative heat transfer enhances the accuracy of reheating simulations [11,12].

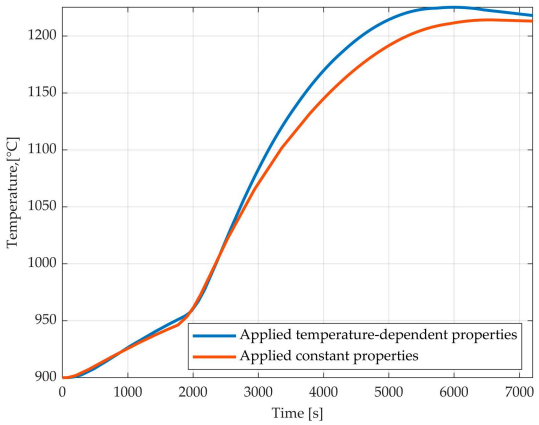


Figure 11. Influence of temperature-dependence and constant properties.

4. Conclusions

In this study, a transient two-dimensional finite element model was successfully developed using COMSOL Multiphysics to simulate the reheating process of continuous casting rail steel blooms prior to hot rolling. The model incorporated temperature-dependent thermophysical properties together with coupled convective and radiative boundary conditions under a three-zone furnace schedule consisting of preheating, heating, and soaking zones. The simulation results demonstrated that radiation is the dominant heat transfer mechanism during high-temperature reheating, while conduction governs internal heat diffusion from the surface toward the bloom core. Significant temperature gradients were observed during the preheating and heating zones; however, these gradients progressively diminished during the soaking period. After 7200 s of heating, the bloom center reached approximately **1218–1220 °C** satisfying rail rolling requirements. The final temperature difference within the cross-section, $\Delta T \approx 6.43$ °C, indicates excellent thermal homogenization, well below the acceptable industrial limit, $\Delta T \leq 50$ °C. Furthermore, incorporating temperature-dependent material properties improved the realism and predictive capability of the model, leading to more accurate estimation of temperature gradients and discharge conditions. The results confirm that proper adjustment of furnace temperature setpoints and soaking duration plays a critical role in achieving uniform internal temperatures and minimizing thermal stress prior to rolling. Overall, the developed numerical framework provides an effective tool for analyzing reheating furnace performance, optimizing thermal schedules, and improving temperature uniformity in rail steel manufacturing.

Author Contributions: Conceptualization, J.R. and S.Z.; methodology, S.Z.; software, S.Z.; validation, S.M., I.S. and P.O.; formal analysis, J.R. and S.Y.S.; investigation, S.Z.; resources, J.R. and S.Z.; data curation, S.Z.; writing—original draft preparation, S.Z.; writing—review and editing, J.R. and S.Ď.; visualization, S.M.; supervision, S.Y.S. and S.Ď.; project administration, J.R.; funding acquisition, J.R. All authors have read and agreed to the published version of the manuscript.

Funding: This research was funded by the KEGA project, grant number 028STU-4/2026, "Implementation of Modern Educational Methods Based on a Scientific and Technical Approach to the Metrological Assurance of Urban Railways". The APC was funded by the same project.

Institutional Review Board Statement: Not applicable.

Informed Consent Statement: Not applicable.

Data Availability Statement: Data will be available on request.

Acknowledgments: During the preparation of this manuscript, the authors used Gemini 2.5 Flash standard version (Google) and ChatGPT-5.5 (OpenAI) for the purposes of language translation, correction, and stylistic editing of non-technical passages. The authors have thoroughly reviewed, edited, and verified the output from both tools and take full responsibility for the content and scientific accuracy of this publication. The authors gratefully acknowledge the support of the Faculty of Mechanical Engineering, Slovak University of Technology in Bratislava, Slovakia; the Faculty of Electro-Mechanics, Kabul Polytechnic University, Kabul, Afghanistan; and the Faculty of Applied Informatics, Tomas Bata University in Zlín, Czech Republic, for their institutional support and cooperation during the preparation of this paper. We acknowledge the support of projects KEGA 028STU-4/2026 and APVV-21-0195, which supported the preparation of this paper.

Conflicts of Interest: The authors declare no conflicts of interest.

References

1. Han, S.; Chang, D.; Kim, C.Y. A numerical analysis of slab heating characteristics in a walking beam type reheating furnace. *Int. J. Heat Mass Transf.* **2010**, *53*, 3855–3861. [CrossRef]
2. Valdes-Tabernero, M.A.; Celada-Casero, C.; Sabirov, I.; Kumar, A.; Petrov, R.H. The effect of heating rate and soaking time on microstructure of an advanced high strength steel. *Mater. Charact.* **2019**, *155*, 109822. [CrossRef]
3. Gu, M.; Chen, G.; Liu, X.; Wu, C.; Chu, H. Numerical simulation of slab heating process in a regenerative walking beam reheating furnace. *Int. J. Heat Mass Transf.* **2014**, *76*, 405–410. [CrossRef]
4. Fang, H.; Wong, M.B.; Bai, Y. Heating rate effect on the thermophysical properties of steel in fire. *J. Constr. Steel Res.* **2017**, *128*, 611–617. [CrossRef]
5. Wang, J.; Liu, Y.; Sundén, B.; Yang, R.; Baleta, J.; Vujanović, M. Analysis of slab heating characteristics in a reheating furnace. *Energy Convers. Manag.* **2017**, *149*, 928–936. [CrossRef]
6. Zarghoon, S.; Emebu, S.; Matušů, R.; Belavý, C.; Bartalský, L.; Ďuriš, S.; Husnain, S.; Mendoza Martinez, C. Full-state feedback LQR with integral gain for control of induction heating of steel billet. *Eng. Sci. Technol. Int. J.* **2024**, *55*, 101721. [CrossRef]
7. Xu, K.; Li, D.; Dou, R.; Yin, H.; Liang, J.; Liu, X.; Wen, Z. Numerical and experimental studies on the heat transfer characteristics and process optimization of the billet soaking furnace. *Appl. Therm. Eng.* **2024**, *253*, 123847. [CrossRef]
8. Liu, Q.; Hanoglu, U.; Rek, Z.; Šarler, B. Simulation of Temperature Field in Steel Billets during Reheating in Pusher-Type Furnace by Meshless Method. *Math. Comput. Appl.* **2024**, *29*, 30. [CrossRef]
9. Ji, W.; Li, G.; Zhang, H.; Guo, X.; Yi, Z.; Wei, L. A novel real-time reconstruction model for transient temperature field of steel billets in the reheating furnace based on mixture-of-experts framework. *Appl. Therm. Eng.* **2025**, *272*, 126434. [CrossRef]
10. Forestier, R.; Costes, F.; Jaouen, O.; Bellet, M. Finite element thermomechanical simulation of steel continuous casting. In Proceedings of the 12th International Conference on Modeling of Casting, Welding and Advanced Solidification Processes (MCWASP XII), Vancouver, BC, Canada, 7–12 June 2009.
11. Hwang, J.-K. Strong Influence of Thermal Properties on Temperature Deviation of Steel Billets During Heating. *SSRN* **2023**. [CrossRef]
12. Ďuriš, S.; Palenčár, R.; Knorová, R. *Metrológia Teploty*, 1st ed.; STU Publishing House: Bratislava, Slovakia, 2013.

Disclaimer/Publisher's Note: The statements, opinions and data contained in all publications are solely those of the individual author(s) and contributor(s) and not of MDPI and/or the editor(s). MDPI and/or the editor(s) disclaim responsibility for any injury to people or property resulting from any ideas, methods, instructions or products referred to in the content.